

Gamma Ray Spectroscopy of an Unknown Radioactive Source

Kellie McGuire^{1,*} and Ronny Nguyen¹

¹*Department of Physics, University of New Hampshire*
(Dated: September 27, 2018)

We identify an unknown radioactive source by measuring its gamma emission spectrum using a NaI scintillator with photomultiplier. To calibrate the experiment we measured the spectra of two known radioactive sources and mapped their energy photopeaks to the channels of a multichannel analyzer. We used this same experimental setup to measure the absorption coefficient of lead at 609 keV. The results of both measurements fall within [...] of published values, validating the experimental methods used.

BACKGROUND AND MOTIVATION

Gamma ray spectroscopy using a NaI detector is a standard method for identifying radioactive substances. The techniques used in gamma ray spectroscopy are thus indispensable to the experimental nuclear physicist, and developing these skills is an important step in training physicists to work in the lab.

Decay of radioactive materials.—Radioactive elements are unstable nuclei that spontaneously decay to lower-energy states, emitting their excess energy in the form of particles and photons. The rate of this decay is governed by quantum mechanics and is probabilistic. The lifetime of a radioactive sample is thus characterized by its half-life: the time necessary for a collection of identical radionuclides to reduce to half their initial number. Given a large enough sample, one can observe this decay directly in the lab.

In general, a radioactive nucleus can undergo many different decays before reaching its final, stable state. These decays are governed by conservation laws, such that only certain decay schemes can occur for a given radionuclide. Further, each possible decay occurs with a definite probability. Radioactive materials can thus be identified by the products of their decay, which act as the signature of the radioactive sample.

Scintillator method.—Scintillating materials are commonly used in radioactive detectors because they emit visible light when struck by charged particles. This light can either be observed directly or translated into energy information, as is done in this experiment.

In the case of gamma ray detection, the incident photon must transfer its energy to a charged particle (electron) before it can be detected by the scintillator. This occurs via three main mechanisms: the photoelectric effect, Compton scattering, and pair production. Whereas in the photoelectric effect and pair production the gamma ray is completely absorbed, in Compton scattering the photon deposits only part of its energy. The recoiling photon is then left to either interact with another electron or escape the detector altogether. As a result, energy

resolution is lost in the region where Compton scattering is dominant. A NaI detector is well-suited for gamma ray spectroscopy because its photoelectric and pair production cross-sections are much larger than its Compton scattering cross-section [1].

EXPERIMENTAL SETUP

A NaI crystal was used to detect gamma rays emitted by the radioactive samples. The NaI crystal was coupled to a photomultiplier, which amplified the resulting photoelectric current through a series of high-voltage dynodes. The amplified current was then converted to a voltage and directed through a spectroscopic amplifier.

The signal was observed on an oscilloscope, and the amplification was increased until it fell just below saturation, corresponding to an output voltage of approximately 4V at the 662 keV photopeak for Cesium-137. This signal was then directed to a multichannel analyzer (MCA), which sorted each pulse (decay event) into a channel according to its amplitude (energy). The emission spectra were then observed and recorded using GammaVision software.

MEASUREMENTS

All measurements were performed in Lab 317 in UNH's DeMeritt Hall, following radiation safety training.

Gamma spectra were recorded on two separate occasions. The second data were necessary because the first data were not adequate for performing the lead attenuation measurement.

For data set 1, seven spectra were recorded: two of known radioactive sources (Cesium-137 and Radium-226), two of unidentified sources, one with a lead attenuator, and two with no source present (background).

For data set 1, each radioactive source was positioned 20 cm in front of the NaI detector “hot end.” This dis-

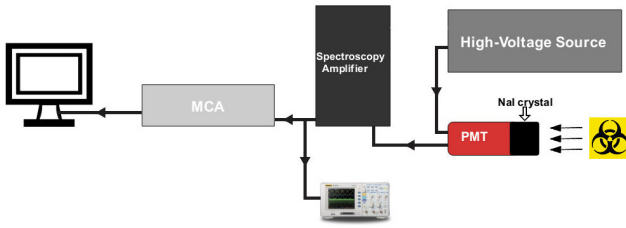


FIG. 1. Experimental setup for gamma ray spectroscopy. A NaI crystal detects gamma emissions from the radioactive source and re-emits them as visible photons. The photons travel to the photomultiplier tube (PMT), where they produce a photoelectric current. This current is accelerated through a series of high-voltage dynodes, which amplifies the current before converting it into a voltage. This voltage is further amplified by the spectroscopic analyzer before reaching the multichannel analyzer (MCA), which sorts each pulse according to its energy.

tance was chosen to optimize the emission cross-section at the detector, permitting the NaI crystal to “see” the maximum number of decay events without exceeding the response time of the detector. The signals from the photomultiplier were amplified by a factor of 500. All spectra were recorded for 200 seconds, except for the second background measurement, which ran for 300 seconds.

An unidentified source labeled “Ore B” was measured, and a quick glance at its spectrum revealed that it was very likely Radium-226. To obtain a true unknown sample, another measurement was made with a different source, labeled “No. 3.”

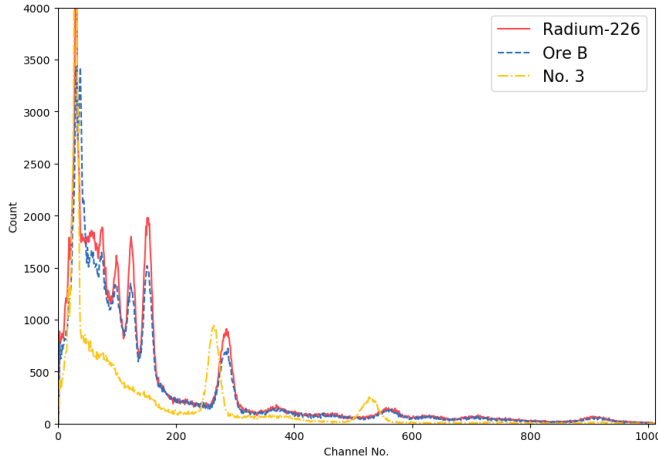


FIG. 2. A visual comparison of Ore B with ^{226}Ra suggests that they are the same radionuclide. To obtain a truly unknown spectrum, No. 3 was also measured.

For data set 2, six spectra were recorded: Cesium-137 and Radium-226, one background, sample No. 3, and two Radium-226 with lead attenuator. Each source was placed 20 cm in front of the detector. The signals

were amplified by a factor of 1000 and recorded for 180 seconds. A different lead absorber (1.25 mm and 7 mm) was used for each of the lead attenuator measurements. For both measurements, the lead absorber was placed midway between the Radium-226 sample and detector hot end.

RESULTS

Calibration—Prior to identifying sample No. 3 and measuring the attenuation coefficient of lead, we calibrated the spectra by mapping the photopeak energies of the two known sources to the channels of the MCA. Because our data were gathered on two separate occasions, it was necessary to perform separate calibrations for each data set. The calibration results for data set 1 are presented here, with results from data set 2 given in the Appendix.

We performed the calibration by first subtracting the recorded background spectrum from the Cesium-137 and Radium-226 spectra and fitting the local background to an exponential plus constant. We then fit the most prominent energy photopeaks to a Gaussian,

$$Ae^{-\frac{(x-X)^2}{2\sigma^2}}, \quad (1)$$

where X represents the MCA channel number of the photopeak max, σ is the width parameter, and A is the amplitude of the photopeak.

The photopeak energies for Cesium-137 and Radium-226 were obtained from [2] and [3], and their errors were taken to be zero. The resulting fit parameters, given in Table I, were used to determine a linear relation between the gamma energies and the channels of the MCA.

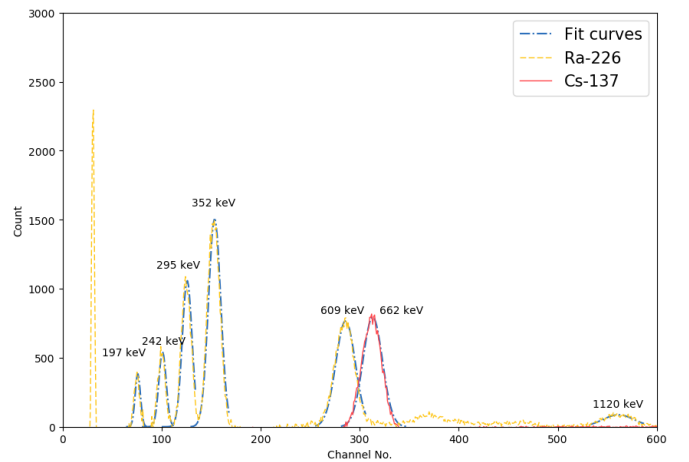


FIG. 3. The most prominent photopeaks of ^{137}Ce and ^{226}Ra were fitted to a Gaussian after removing global and local background noise from the spectra. The photopeak energies were obtained from tables of known decays.

TABLE I. Photopeak Fit Parameters.

Energy (keV)	ADC Channel No.	σ
1120	561	15.75
661.64	313.09	9.84
609.312	285.69	9.81
351.932	153.45	6.20
295.224	125.73	4.95
241.997	100.83	3.72
187.1	75.85	2.67

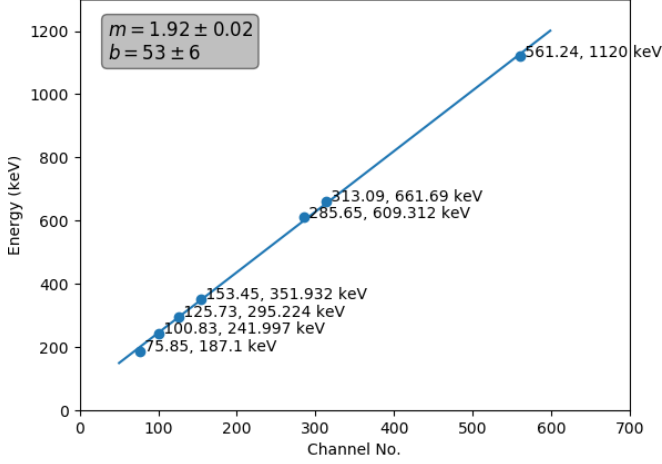


FIG. 4. A plot of known photopeak energies and MCA channel numbers, obtained from fitting the photopeaks to gaussian curves, shows a strong linear relationship in the measured energy range.

Errors on the linear fit parameters were calculated using the following relations from [4]

$$\sigma_b = \sigma_y \sqrt{\frac{\sum_{i=1}^N x_i^2}{\Delta}}, \quad (2)$$

$$\sigma_m = \sigma_y \sqrt{\frac{N}{\Delta}}, \quad (3)$$

$$\sigma_y = \sqrt{\frac{1}{N-2} \sum_{i=1}^N (y_i - b - mx_i)^2}, \quad (4)$$

$$\Delta = N \sum_{i=1}^N x_i^2 - \left(\sum_{i=1}^N x_i \right)^2. \quad (5)$$

Our results indicate an offset of 53 ± 5.9 keV for our energy axis, with a resolution of 1.92 ± 0.02 keV per channel, or a relative resolution of $6.0 \pm 0.32\%$, which we calculated from

$$\frac{1}{n} \left(\sum_{i=1}^n \frac{2m\sigma_i}{E_i} \right) \times 100, \quad (6)$$

where σ is the width parameter of the peak, E is the photopeak energy, and n is the number of photopeaks measured.

With these results, we calibrated our spectra by plotting them on our new energy axis, as shown in Fig. IV.

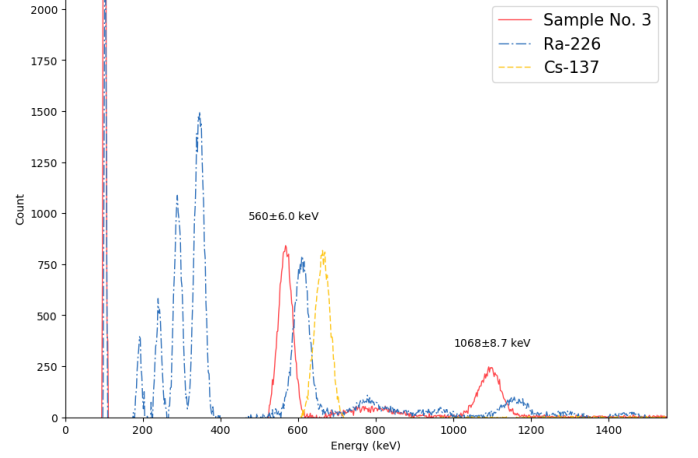


FIG. 5. Gamma spectra with energy calibration.

Lead attenuation of Radium-226—As mentioned in the Measurements section, it was necessary to obtain a second set of spectra, as the first data did not contain enough information to measure the absorption coefficient of lead. The calibration results for data set 2 are given in the Appendix.

Lead absorbers of two different thicknesses (1.25 mm and 7 mm) were used to attenuate the gamma spectra of Radium-226.

A background spectrum was subtracted from the Radium-226 spectra, which were then fitted to an exponential term plus constant to remove any remaining background. The 609 keV photopeaks of Radium-226 were then fitted to a Gaussian,

$$Ae^{\frac{-(x-X)^2}{2\sigma^2}}. \quad (7)$$

The total number of decay events under each fit was calculated using a simple function that summed the total area under each curve, the results of which are presented in Table II. Errors for the counts were calculated using the fitting errors of A and σ .

We used these results to calculate the absorption coefficient for lead and the mass attenuation of lead, using

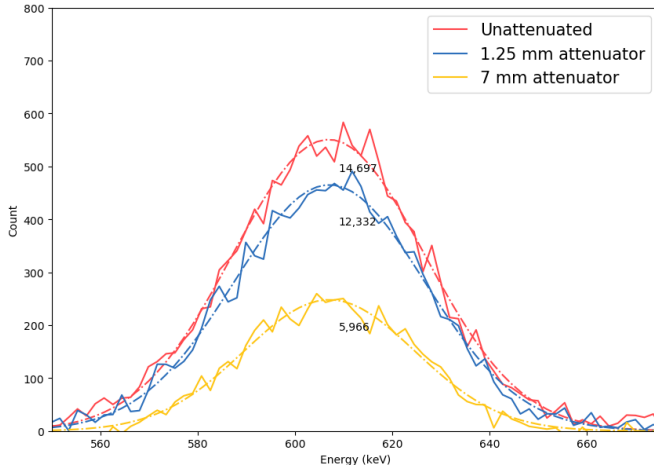


FIG. 6. Lead attenuation of the 609 keV photopeak of ^{226}Ra , showing the total number of counts under each curve.

TABLE II. Lead attenuation of 609 keV gamma rays.

Source	I (count)	δI
^{226}Ra unattenuated	14,697	2,578
With 1.25 mm absorber	12,332	2,570
With 7 mm absorber	5,966	2,435

$$I(x) = I_0 e^{-\mu x}, \quad (8)$$

where I and I_0 are the attenuated and unattenuated

counts under the curves, x is the thickness of the absorber, and μ is the attenuation coefficient. For the mass density of lead, ρ , we used 11.34 g cm^3 and assumed no error in this value. To calculate the error in our results, we considered uncertainties in the counts under both curves, as well as in the thickness of the absorbers. Our results show $0.14 \pm 0.22 \text{ cm}^2/\text{g}$ for the 1.25 mm absorber and $0.129 \pm 0.064 \text{ cm}^2/\text{g}$ for the 7 mm absorber. [Note to reviewer: clearly there are problems with the first measurement, as the error is larger than the calculation.] The large error in the 1.25 mm measurement suggests a flaw in the experimental setup, possibly the result of using an uneven absorber whose true thickness was difficult to measure. The result from the 7 mm absorber is in close agreement with the value of $0.1248 \text{ cm}^2/\text{g}$ for 600 keV radiation, found in [5].

Identity of unknown sample—

CONCLUSIONS AND REMARKS

* kjm1042@wildcats.unh.edu

- [1] W.R. Leo, *Techniques for Nuclear and Particle Physics Experiments: A How-to Approach* (1994).
- [2] <https://www.cpp.edu/~pbsiegel/bio431/gennergies.html>
- [3] Radiochemistry Society www.radiochemistry.org/periodictable/gam
- [4] John R. Taylor, *An Introduction to Error Analysis: The Study of Uncertainties in Physical Measurements* (1997).
- [5] <https://physics.nist.gov/PhysRefData/XrayMassCoef/ElemTab/z8>